São Paulo J. Math. Sci. (2018) 12:82–107
https://doi.org/10.1007/s40863-017-0078-4

Minimal time splines on the sphere

Teresa Stuchi[1] · **Paula Balseiro**[2] · **Alejandro Cabrera**[3] · **Jair Koiller**[4]

Published online: 27 November 2017
© Instituto de Matemática e Estatística da Universidade de São Paulo 2017

Abstract An interesting problem in geometric control theory arises from robotics and space science: find a smooth curve, controlled by a bounded acceleration, connecting in minimum time two prescribed tangent vectors of a Riemannian manifold Q. The state equation is $\nabla_{\dot\gamma}\dot\gamma = u \in TQ$, $|u| \leq A$. Applying Pontryagin's principle one gets a Hamiltonian system in $T^*(TQ)$. We consider this problem in $S^2(r)$. Seemingly, it has not been addressed before. Via the $SO(3)$ symmetry, we reduce the four degrees of

Dedicated to Waldyr Muniz Oliva.

Supported by Capes/CNPq/CsF 089-2013.

✉ Jair Koiller
jairkoiller@gmail.com

Teresa Stuchi
tstuchi@if.ufrj.br

Paula Balseiro
pbalseiro@vm.uff.br

Alejandro Cabrera
acabrera@labma.ufrj.br

1 Departamento de Física Matemática, Universidade Federal do Rio de Janeiro, Centro de Tecnologia - Bloco A - Cidade Universitária - Ilha do Fundão, Rio de Janeiro, RJ 21941-972, Brazil

2 Departamento de Matemática Aplicada, Universidade Federal Fluminense, Rua Mário Santos Braga, S/N, Campus do Valonguinho, Niterói, RJ 24020-140, Brazil

3 Departamento de Matemática Aplicada, Universidade Federal do Rio de Janeiro, Centro de Tecnologia - Bloco C - Cidade Universitária - Ilha do Fundão, Rio de Janeiro, RJ 21941-972, Brazil

4 Departamento de Matemática, Universidade Federal de Juiz de Fora Campus Universitário, Juiz de Fora, MG 36036-900, Brazil

freedom system to the five variables (a, v, M_1, M_2, M_3), where v is the scalar velocity, conjugated to a costate variable a and (M_1, M_2, M_3) are costate variables that satisfy $\{M_i, M_j\} = \epsilon_{ijk} M_k$. We derive the reduced equations and find special analytical solutions, that are organizing centers for the dynamics. Reconstruction of the curve $\gamma(t)$ is achieved by a time dependent linear system of ODEs for the orthogonal matrix R whose first column is the unit tangent vector of the curve and whose last column is the unit normal vector to the sphere.

Keywords Riemannian splines · Geometric control · Reduction · Reconstruction

Mathematics Subject Classification 53D20 · 65D07 · 49J15 · 70H06

1 Introduction

The *rendezvous problem* from robotics and space science consists of planning a path with prescribed initial and final position and velocities [1–3]. Achieving, for instance, a smooth docking of a service spacecraft to the International Space Station or fetching a satellite.[1]

Mechanical control problems were first studied via Geometric Mechanics in Andrew Lewis thesis with Richard Murray at Caltech [5]. The standard reference is [6], a treatise by Bullo and Lewis. The organism or device is modeled by a configuration space Q, together with a metric (kinetic energy) governing its inertia. Acting external and internal forces produce an acceleration, interpreted as the control u that produces deviation from geodesic motion.

If ∇ denotes the Levi–Civita connection, the state equation is

$$\nabla_{\dot{q}} \dot{q} = u. \tag{1}$$

The aim is to connect two tangent vectors (q_o, v_o) and (q_1, v_1) minimizing a cost functional. Such curves are called *variational splines*. Via Pontryagin's principle, every cost functional associated to (1) yields a Hamiltonian system in $T^*(TQ)$.

Two cases have received special attention. The first case concerns *cubic splines* (also called L^2), that were introduced around 1990 [7,8]. They minimize

$$\int_0^T \frac{\beta}{2} |u|^2 \, dt \tag{2}$$

with a prescribed time T besides the starting and end tangent vectors. Cubic splines have been recently used in longitudinal studies in medical imaging. The research area is called *computational anatomy* [9–12].

[1] Warning: this is a spoiler. A thrilling *rendez-vous* example is the rescue of astronaut Mark Watney (Matt Damon) by Melissa Lewis (Jessica Chastain) in the movie 'The Martian', directed by Ridley Scott, based on the novel by Weyr [4].

The second case is *the time minimal problem*, that has been used frequently for path planning in robotics and space science.[2] In the Markov–Dubins problem, the acceleration is always normal to the path, so in this case minimal time is equivalent to minimal length. There is a vast literature on this classical problem. More recently, some authors allowed a tangential acceleration in addition to a normal component. This was called *dynamic Markov–Dubins* in [15]. It consists in connecting two vectors in minimum time, under the restriction

$$|u| \leq A, \quad \text{where } A \text{ is a prescribed bound.} \tag{3}$$

This paper is a follow up of [16], where we presented a geometric formulation for variational problems with state space TQ, or more generally with a state space A that is an anchored vector bundle over Q, so that T^*A is a double bundle.

A connection in the bundle $A \to Q$ allows to rewrite the canonical symplectic form on $T^*(TQ)$ (resp. T^*A) using a convenient splitting of covectors. Among the examples, we discussed cubic splines on spheres.

Here we continue the study, focusing on the second case: time minimal splines on $S^2(r)$. In Sect. 2 we contextualize the problem. We apply Pontryagin's method in its standard formulation, embedding $TS^n(r)$ in $\Re^{n+1} \times \Re^{n+1}$. Then we introduce modified costate variables allowing to write the equations of motion for the optimal Hamiltonian in a very geometric fashion.

The core of the paper is Sect. 3. Following [16], in the case $n = 2$ we make a special construction, using a diffeomeorphism of $TS^2(r) - 0$ to $SO(3) \times \Re_+$, with coordinates (R, v). The last column of the orthogonal matrix R is the unit normal vector to the sphere, and the first is the normalized tangent vector of the spline.

The coordinate v is the scalar velocity, conjugated to a costate variable a, that acts on the tangential acceleration, and (M_1, M_2, M_3) are costate variables that act on the frame rotations $R^{-1}\dot{R}$. These momenta satisfy $\{M_i, M_j\} = \epsilon_{ijk} M_k$.

We derive the reduced hamiltonian and find two families of special analytical solutions, that are organizing centers for the dynamics. One of the families trace the equators, exhibiting there the bang-bang phenomenon. The other family is formed by circles with geodesic curvature $1/r$, that can be traversed both ways. They were found by unreduction, and appear in pairs forming figure eights.

In Sect. 4 we compute the equilibria of the reduced system and show that they are of loxodromic type, as it also happened for cubic splines. Section 5 makes a digression on the 1-dimensional case of time minimal trajectories along equators. In Sect. 6 we reconstruct the trajectories of the unreduced system corresponding to the equilibria of the reduced system in Sect. 4. A benchmark numerical simulation, using the free software BOCOP, developed at INRIA, is presented in Sect. 7. Section 8 we discuss some loose ends and present some research directions.

We end this introduction with additional references about variational splines in medical imaging. In computational anatomy cubic splines have been used for lon-

[2] The time minimal-bounded acceleration problem is almost always equivalent to the so called L^∞ control problem considered recently by Noakes and Kaya [13,14], where they ask for a trajectory that minimizes the sup of the norms of the accelerations, with fixed transition time.

gitudinal medical studies [10–12] and for interpolation and statistics on manifolds [17–24]. We observe that a tangent vector gives a minimal model for a *short process*. The idea of comparing two short physiological processes using splines is not yet much explored. This question is important in embryology, where it is called morphokinetics [25].

2 Simple splines in $S^n(r)$: the minimal time problem

As observed by Chang [26], a dynamic optimization problem whose state space is a manifold can be conveniently formulated using embeddings on an Euclidian space. We embed TS^n in $\mathbb{R}^{n+1} \times \mathbb{R}^{n+1}$ and write the state equations so that it has TS^n as an invariant submanifold. This allows us to apply Pontryagin's principle in the usual way. We fix a sphere $S^n(r)$ of radius r. The state equations are

$$\dot{x} = \mathbf{v}, \quad \dot{\mathbf{v}} = u - |\mathbf{v}|^2 x/r^2, \quad u \perp x \tag{4}$$

Here u, the tangential component of the acceleration vector, is the control. The second term in the right hand side of the equation for $\dot{\mathbf{v}}$ is the normal acceleration required to keep the trajectory in the sphere. Hence these equations have the tangent bundle of the sphere of radius r as invariant submanifold. We used boldface only for the tangent vector $\mathbf{v}$ because $v = |\mathbf{v}|$.

2.1 Applying Pontryagin Maximum Principle on $\mathbb{R}^{2(n+1)}$

We now formulate the problem. Let

$$((x, \mathbf{v}), (\tilde{p}_x, \tilde{p}_v)) \in T^*(T\mathbb{R}^{n+1}) = \mathbb{R}^{4(n+1)}$$

with the canonical form

$$\Omega_{T^*(T\mathbb{R}^{n+1})} = d\tilde{p}_x \wedge dx + d\tilde{p}_v \wedge d\mathbf{v}. \tag{5}$$

We have the Hamiltonian family:

$$H^u = -1 + \tilde{p}_x \cdot \mathbf{v} + \tilde{p}_v \cdot \left(u - \frac{|\mathbf{v}|^2}{r^2} x \right).$$

We obtain the optimal control (using $u \perp x$)

$$u^* = A \frac{p_v^{\parallel}}{|p_v^{\parallel}|} \tag{6}$$

where

$$p_v^{\parallel} = \tilde{p}_v - \langle \tilde{p}_v, x \rangle x/r^2 \tag{7}$$

is the projection of $\tilde{p}_v$ on tangent plane of the sphere. The case $p_v^{\|} = 0$, needs special attention and is discussed in the conclusion section. Substituting back in the Hamiltonian family we get

Proposition 1 *The optimal Hamiltonian for the time minimal splines in $S^n(r)$*

$$H^* = -1 + \tilde{p}_x \cdot \mathbf{v} + A\,|p_v^{\|}| - \tilde{p}_v \cdot \frac{|\mathbf{v}|^2}{r^2}\, x. \tag{8}$$

where we use standard symplectic structure (5)*, with initial conditions such that*

$$|x| = r, \quad \mathbf{v} \perp x.$$

2.2 Using split costate variables

The fact that the covectors $\tilde{p}_x, \tilde{p}_v$ are arbitrary vectors in $\Re^{n+1}$ is a nuisance: each contains one spurious dimension. Define modified costate variables p, α by

$$\alpha = p_v^{\|} = \tilde{p}_v - \langle \tilde{p}_v, x\rangle x/r^2 \tag{9}$$

$$p = \tilde{p}_x^{\|} - \frac{\langle \tilde{p}_v, x\rangle}{r^2}\,\mathbf{v} \tag{10}$$

Note that if $|x| = r$ and $\mathbf{v} \perp x$ then p, α are also in $T_x S^n(r)$. In fact, as follows from the theory in [16], these modified costate variables represent a splitting for a covector $P_{(x,\mathbf{v})} \in T^*_{(x,\mathbf{v})}\, T S^n(r))$, achieved via the Levi–Civita connection in the tangent bundle $T S^n$. The Hamiltonian (8) gets a simpler expression:

$$H^* = -1 + p \cdot \mathbf{v} + A\,|\alpha|. \tag{11}$$

There is a price: the symplectic form in the variables $(x,\ p, \mathbf{v}, \alpha)$ is non-canonical. It has extra terms, arising from the connection, but they have a geometric content. For any Hamiltonian $H(x,\ p, \mathbf{v}, \alpha)$, the resulting equations can be conveniently written as follows:

Proposition 2 *Hamiltonian equations with split momenta p, α:*

$$\begin{bmatrix} \dot{x} \\ \nabla_{\dot{x}} p \\ \nabla_{\dot{x}} v \\ \nabla_{\dot{x}} \alpha \end{bmatrix} = \begin{bmatrix} 0 & I & 0 & 0 \\ -I & 0 & 0 & R(\cdot, v)v \\ 0 & 0 & 0 & I \\ 0 & -R(\cdot, v)v & -I & 0 \end{bmatrix} \begin{bmatrix} H_x \\ H_p \\ H_{\mathbf{v}} \\ H_\alpha \end{bmatrix} \tag{12}$$

where R is the curvature tensor of the metric on Q.

Indeed, we showed in [16] that these equations also hold for any metric on a Riemannian manifold, via the splitting p, α of covectors P_{v_x} induced by its Levi–Civita connection. In the case of the unit sphere ($r = 1$) the curvature tensor is given by

$$R(X, Y)Z = (Y \cdot Z)X - (X \cdot Z)Y \tag{13}$$

For the time-minimal problem, we use the Hamiltonian (11) so that

$$H_x = 0, \quad H_p = \mathbf{v}, \quad H_{\mathbf{v}} = p, \quad H_\alpha = A\alpha/|\alpha| \tag{14}$$

Explicitly

$$\dot{x} = \mathbf{v}, \quad \nabla_{\dot{x}}\mathbf{v} = A\alpha/|\alpha|, \ \nabla_{\dot{x}}\alpha = -p, \nabla_{\dot{x}}\, p = R(A\alpha/|\alpha|, \mathbf{v})\mathbf{v}. \tag{15}$$

For cubic splines on an arbitrary Riemannian manifold Q have the optimal Hamiltonian $H^* = -(1/2)\beta|u|^2 + p\cdot\mathbf{v} + \alpha\cdot u$. It follows from (12) that the solution curves satisfy the Crouch–Leite equations [27],

$$\nabla^3_{\dot{x}}\dot{x} = -R(\nabla_{\dot{x}}\dot{x}, \dot{x})\dot{x}. \tag{16}$$

In contradistinction, in the time-minimal case, it seems that it is not possible to write (15) a single third order equation.

3 Convex surfaces: reduction and reconstruction equations

We recall the construction that we did in [16] of coordinates (a, v, M_1, M_2, M_3, R) in $T^*(TS^2 - 0)$, with $v > 0$, $R \in SO(3)$. The zero section must be excluded. For a closed smooth convex surface $\Sigma \subset \mathbb{R}^3$, the Gauss map induces a diffeomorphism between $T\Sigma - 0$ and $\mathbb{R}^+ \times SO(3)$:

$$\mathbf{v}_q \ \leftrightarrow (v, R), \quad v = ||\mathbf{v}_q|| \neq 0 \tag{17}$$

$R \in SO(3)$ is constructed as follows: via the Gauss map, a point $q \in \Sigma$ correspond uniquely to an external unit normal vector to the surface, which we denote e_3.. Now, a nonzero tangent vector $\mathbf{v}_q$ corresponds uniquely to a pair (v, e_1) with $v = |\mathbf{v}_q|$, $|e_1| = 1$. so $\mathbf{v}_q = v\, e_1$, $v > 0$. We use a redundant vector $e_2 = e_3 \times e_1$ to construct the matrix R with columns e_1, e_2, e_3. Now recall the Darboux formulas

$$e_1' = \kappa_g\, e_2 + \kappa_n\, e_3, \quad e_2' = -\kappa_g\, e_1 + \tau_g\, e_3, \quad e_3' = -\kappa_n\, e_1 - \tau_g\, e_2 \quad (' = d/ds)$$

where κ_g is the geodesic curvature, κ_n the normal curvature, and τ_g the geodesic torsion of a curve γ in the surface. These formulas can be rewritten as

$$\dot{R} = R\,X, \quad X = v \begin{pmatrix} 0 & -\kappa_g & -\kappa_n \\ \kappa_g & 0 & -\tau_g \\ \kappa_n & \tau_g & 0 \end{pmatrix}. \tag{18}$$

The normal curvature κ_n cannot be a a control variable, since it corresponds to the constraining force to the surface. In fact, taking derivatives in the ambient space,

$$\ddot{\gamma} = \dot{v}\, e_1 + v^2\, e_1' = u_1\, e_1 + v^2(\kappa_g\, e_2 + \kappa_n\, e_3) = \nabla_{\dot{\gamma}}\, \dot{\gamma} + v^2\kappa_n\, e_3$$

with

$$\kappa_n = (e_1', e_3) = -(e_3', e_1) := B(e_1, e_1)$$

where B is the second fundamental form of the surface.

3.1 State equations

We then write the state equation in terms of the Levi–Civita connection,

$$\nabla_{\dot\gamma}\,\dot\gamma = u_1\, e_1 + u_2 e_2 \tag{19}$$

where u_1, u_2 are the controls. This calculation above also shows that

$$u_1 = \dot v, \quad u_2 = v^2 \kappa_g. \tag{20}$$

For the geodesic torsion, Darboux found the interesting formula

$$\tau_g = \tau_g(e_1) = (\kappa_1 - \kappa_2)\sin\phi\,\cos\phi \tag{21}$$

where ϕ is the angle between the unit tangent vector e_1 to the curve and a principal direction on the surface. In conclusion, the state equations can be written as

Proposition 3

$$\dot v = u_1, \quad \dot R = R\,X \tag{22}$$

with

$$X = \begin{pmatrix} 0 & -u_2/v & -v\,B(e_1,e_1) \\ u_2/v & 0 & -v\,\tau_g(e_1) \\ v\,B(e_1,e_1) & v\,\tau_g(e_1) & 0 \end{pmatrix}. \tag{23}$$

3.2 Hamiltonian for time minimal splines on the sphere

For an arbitrary convex surface, the state equations are coupled, but for the sphere, the dependence of X on e_1 disappears. Darboux formula (21) shows that the geodesic torsion vanishes identically on any spherical curve.
Thus our convention gives a negative sign for the normal curvature in the sphere. Consider a spherical curve $\gamma(t)$, that is $\gamma(t)\cdot\gamma(t) \equiv r^2$. Differentiating twice results $(\ddot\gamma, \gamma) = -(\dot\gamma, \dot\gamma)$, i.e., $(\ddot\gamma, e_3) = -v^2/r$, so that $\kappa_n = -1/r$. The state equations for the sphere are therefore (22, 23) with

$$X = \begin{pmatrix} 0 & -u_2/v & v/r \\ u_2/v & 0 & 0 \\ -v/r & 0 & 0 \end{pmatrix} \tag{24}$$

The skew-symmetric matrix $X \in so(3)$ can be conveniently represented as

$$\Omega = (0, v/r, u_2/v). \tag{25}$$

We introduce costates (a, M), $a \leftrightarrow v$ and $M = (M_1, M_2, M_3) \leftrightarrow \Omega = (\Omega_1, \Omega_2, \Omega_3)$, with commutation relations

$$\{a, v\} = 1, \{M_i, M_j\} = \epsilon_{ijk} M_k. \tag{26}$$

The Hamiltonian family is given by

$$H = -1 + a \cdot u_1 + M_2\, v/r + M_3 \cdot u_2/v. \tag{27}$$

Maximizing (27) taking into account that

$$u_1^2 + u_2^2 \leq A^2.$$

results in

Proposition 4 *The time minimal problem in the sphere $S^2(r)$ in state variables (v, R) and costates (a, M) has optimal controls*

$$u_1^* = A\, a/\sqrt{a^2 + M_3^2/v^2}, \quad u_2^* = A\, M_3/\left(v\sqrt{a^2 + M_3^2/v^2}\right). \tag{28}$$

The optimal Hamiltonian is given by

$$H = -1 + A\sqrt{a^2 + M_3^2/v^2} + M_2 v/r \tag{29}$$

with commutators $\{a, v\} = 1, \{M_i, M_j\} = \epsilon_{ijk} M_k$. The reconstruction equations are $\dot{R} = R\, X$ with

$$X = X(M_3, a, v) = \begin{pmatrix} 0 & -u_2^*/v & v/r \\ u_2^*/v & 0 & 0 \\ -v/r & 0 & 0 \end{pmatrix}. \tag{30}$$

The reduced equations of motion are given by

$$\begin{aligned} \dot{v} &= u_1^* = aA/\sqrt{a^2 + M_3^2/v^2} \\ \dot{a} &= -M_2/r + \frac{AM_3^2}{v^3\sqrt{a^2 + M_3^2/v^2}} \\ \dot{M} &= \det \begin{pmatrix} i & j & k \\ M_1 & M_2 & M_3 \\ 0 & v/r & \frac{AM_3}{v^2\sqrt{a^2+M_3^2/v^2}} \end{pmatrix} \end{aligned} \tag{31}$$

Clearly we have a Casimir

$$\mu^2 = M_1^2 + M_2^2 + M_3^2. \tag{32}$$

We have shown in [16] that the Poisson map from unreduced variables $(x, \mathbf{v}, p, \alpha)$, where $x \in S^2$ $(r = 1, \mathbf{v}, p, \alpha \perp x)$ to the reduced variables (a, v, M_1, M_2, M_3), is

$$\begin{aligned} a &= \alpha \cdot \mathbf{v}/v, \quad v = |\mathbf{v}| \\ M_1 &= \det(p, \mathbf{v}/v, x) \\ M_2 &= p \cdot \mathbf{v}/v \\ M_3 &= \det(\alpha, x, \mathbf{v}) \end{aligned} \tag{33}$$

4 Relative equilibria: stability analysis

By definition, relative equilibria of the full system in $T^*(TS^2)$ are the equilibria of the reduced system. Let's find them. From the $(\dot{a}, \dot{v})$ equations we get:

$$\text{(i)} \quad a = 0, \quad M_2 = \frac{Ar}{v^2 \text{sign}(v)} |M_3|$$

From the $\dot{M}$ equations we get either $M_3 = 0$ (this case will be discussed below) or, if $M_3 \neq 0$,

$$\text{(ii)} \quad M_2 = \frac{v^3}{Ar} \sqrt{a^2 + M_3^2/v^2}$$

Using these two informations we get, if $M_3 \neq 0$

$$M_2/|M_3| = \frac{Ar}{v^2 \text{sign}(v)} = \frac{v^2 \text{sign}(v)}{Ar}$$

Therefore

$$v = \pm\sqrt{rA}, \quad M_2/|M_3| = \text{sign}(v), \quad \text{signM}_2 = \text{sign}(v) \tag{34}$$

where we allow the variable v to have a negative sign as well. Note that the dimensions are correct:

$$A \sim L/T^2, \quad r \sim L \Rightarrow |v| = \sqrt{Ar} \sim L/T$$

Proposition 5 *The equilibria of reduced system are*

$$\begin{aligned} a = 0, \quad v = \pm\sqrt{rA} \\ M = \mu\left(0, \sqrt{2}/2, \pm\sqrt{2}/2\right) \quad \text{if} \quad v > 0 \\ M = \mu\left(0, -\sqrt{2}/2, \mp\sqrt{2}/2\right) \quad \text{if} \quad v < 0 \end{aligned} \tag{35}$$

that live in the Casimir sphere

$$\mu^2 = 2A/r. \tag{36}$$

The relation (36) follows from (30). The reconstructed $R(t)$ is therefore the product of $R(0)$ (to the left) followed by rotation around the unit vector

$$\left(0, \text{sign}(v)/\sqrt{2}, \text{sign}(M_3)/\sqrt{2}\right). \tag{37}$$

with angular velocity

$$\omega = \sqrt{2A/r}\,. \tag{38}$$

In order to proceed to the stability analysis, it is useful to give a symplectic version of the Poisson system (31). We introduce spherical coordinates in the momentum sphere $|M| = \mu$:

$$\begin{aligned} M = \mu\,(\cos\phi\cos\theta, \sin\phi, \cos\phi\sin\theta) \\ (-\pi \le \theta \le \pi, \quad -\pi/2 \le \phi \le \pi/2) \end{aligned} \tag{39}$$

so that the optimal Hamiltonian becomes

$$H = \mu\sin\phi\, v/r + A\sqrt{a^2 + \mu^2(\cos\phi)^2\,(\sin\theta)^2/v^2} \tag{40}$$

Setting $z = \sin\phi$ we get

Proposition 6 *Symplectic description of the reduced system*

$$H = \mu\, zv/r + A\sqrt{a^2 + \mu^2(1 - z^2)\,(\sin\theta)^2/v^2} \tag{41}$$

$$\Omega = da \wedge dv + \mu dz \wedge d\theta, \quad dz = \cos\phi\, d\phi \tag{42}$$

with $-1 \le z \le 1, \theta \in \Re \bmod 2\pi$.

There are three discrete symmetries [16], that can be explored in future work: velocity reversal (changing signs in all variables), time reversal, and left–right.[3] The equilibria

[3] In the unreduced problem it means that any trajectory can be flipped about a tangent vector at any time.

are

$$\begin{aligned} &a = 0, \quad v = \pm\sqrt{Ar} \\ &v > 0: \quad \theta = \pm\pi/2, \phi = \pi/4 \quad (z = \sqrt{2}/2) \\ &v < 0: \quad \theta = \pm\pi/2, \phi = -\pi/4 \quad (z = -\sqrt{2}/2) \end{aligned} \tag{43}$$

The equations of motion in variables (a, v, z, θ) are given by

$$\begin{aligned} \dot{a} &= -H_v = -\mu z/r + \frac{\mu^2 A(1-z^2)(\sin\theta)^2}{v^3\sqrt{P}} \\ \dot{v} &= H_a = Aa/\sqrt{P} \\ \mu\dot{z} &= -H_\theta = -\mu^2 A\,(1-z^2)\sin\theta\cos\theta\,/\left(v^2\sqrt{P}\right) \\ \mu\dot{\theta} &= H_z = \mu v/r - \mu^2 A\, z\,(\sin\theta)^2/(v^2\sqrt{P}) \end{aligned} \tag{44}$$

where

$$P = a^2 + \mu^2(1-z^2)\,(\sin\theta)^2/v^2.$$

We computed the linearization matrix of the system at the four equiilibria (35) [equivalently (43)] with $\mu = \sqrt{2A/r}$ (36). These four matrices are all equal; the calculation is summarized in the "Appendix A". We get, in the order (a, v, z, θ):

$$L = \begin{bmatrix} 0 & 2/r^2 & 2\sqrt{2Ar} & 0 \\ -Ar & 0 & 0 & 0 \\ 0 & 0 & 0 & -\sqrt{A/(2r)} \\ 0 & -2/r & 2\sqrt{2}\sqrt{A/r} & 0 \end{bmatrix} \tag{45}$$

The characteristic polynomial is

$$p(\lambda) = \lambda^4 + 4\,\frac{A}{r}\,\lambda^2 + 8\,\frac{A^2}{r^2} \tag{46}$$

Proposition 7 *The eigenvalues at the four equilibria all equal, of loxodromic type, and are given by*

$$\lambda = \mu\left(\pm\sqrt{(\sqrt{2}-1)/2} \pm i\sqrt{(\sqrt{2}+1)/2}\right) \quad \text{with} \quad \mu = \sqrt{2A/r} \tag{47}$$

5 The problem in S^1

We now discuss the case $M_1 = M_3 \equiv 0$, $M_2 = \text{const} \neq 0$. Equations (31) yield

$$\dot{a} = -M_2/r, \quad \dot{v} = A\,\text{sign}(a) \tag{48}$$

This shows that $a(t)$ is a linear function, and $\dot{v} = \pm A$ according to the sign of a, that changes sign just once since we assumed $M_2 \neq 0$. In turn, (30) gives $\dot{R} = R\,X$ with

$$X = X(M_3, a, v) = \begin{pmatrix} 0 & 0 & \frac{v}{r} \\ 0 & 0 & 0 \\ -\frac{v}{r} & 0 & 0 \end{pmatrix}. \tag{49}$$

Thus the reconstruction of $R(t)$ is given by an initial R(0) multiplied on the right by a rotation around the second axis. If $R(0) = I$ then the tracing point traverses a circle in the x-z plane starting in the north pole of the sphere. Since $R(0)$ is arbitrary, all great circles are covered.

This makes sense. Solutions of the time minimal problem in S^1 are embedded among the solutions of the S^2 problem. The problem in S^1 can be thought as a collection of time minimal problems in $\Re$, its universal cover, where the initial and final positions are separated by integer multiples of 2π. The problem in $\Re$ is a paradigmatic example for *bang-bang solutions* (eg. [28], chapter 14.5).

Examining equations (44) is also instructive. This case corresponds to $z = \pm 1$. We have

$$\dot{a} = -\mu\,\mathrm{sign}(z)/r, \quad \dot{v} = A\mathrm{sign}(a)$$

which coincides with the above equations, since $M_2 = \mu\,\mathrm{sign}(z)$. The other equations are $\dot{z} = 0$ and

$$\dot{\theta} = v/r - \frac{\mu A \mathrm{sign}(z)}{v^2|a|}$$

Although this equation is irrelevant for $z \equiv \pm 1$, since the 'latitude' θ is void of meaning at $\phi = \pm\pi/2$, it carries some information. It is discontinuous and tends to infinite as $v \to 0$. Nearby solutions, although smooth, should be highly complex. Finally, there is the case $\mu = 0$. In this case there is no bang-bang: the physical path is uniformly accelerated along an equator.

6 Reconstructed trajectories corresponding to relative equilibria

We obtain exactly the same "figure eight " paths in the sphere $S^2(r)$ as in the case of cubic splines analysed in [16]. For completeness, we summarize the calculation here, making some simple adaptations. First we observe that relation (28) for $u_2^* = v^2\kappa_g$ implies that the reconstructed trajectories satisfy

$$|\kappa_g| = \frac{1}{r}. \tag{50}$$

Now we recall that on a sphere of radius r, the parallel of latitude α has geodesic curvature $\kappa_g = \tan\alpha/r$. Thus in our case $\alpha = \pi/4$.

Proposition 8 *Figure eights. The reconstructed curves in S^2, corresponding to the two equilibria, with $R(0) = I$, are two orthogonal (touching) circles making a 45° angle with the equatorial plane. They are given by*

$$\gamma(t) = r\left(\frac{\sqrt{2}}{2}\sin\theta, \pm\frac{1}{2}(1-\cos\theta), \frac{1}{2}(1+\cos\theta)\right) \tag{51}$$

with

$$\theta = \sqrt{2}\,\frac{v}{r}\,t, \quad |v| = \sqrt{Ar} \tag{52}$$

Proof As in [16] we have steady rotations about the unit vectors

$$(u_x, u_y, u_z) = \left(0, \frac{\sqrt{2}}{2}, \pm\frac{\sqrt{2}}{2}\right)$$

with angular velocity $\omega = \pm\sqrt{2}\,v/r$. The result is the same, but the calculations is slightly different here. Recall that $X(M_3, a, v)$ is given by (30), the infinitesimal rotations

$$(0, -v/r, A\,M_3/(v^2\sqrt{a^2 + M_3^2/v^2})$$

We substitute $a = 0$, $A = v^2/r$, so that the third entry is

$$(v^2/r)\,\mathrm{sign}(M_3)/|v| = \mathrm{sign}(M_3)|v|/r.$$

Now we recall from [16] that for an unit vector (u_x, u_y, u_z) the rotation matrix $R(\theta)$ with $R(0) = I$ is given by

$$\begin{bmatrix} \cos\theta + u_x^2(1-\cos\theta) & u_xu_y(1-\cos\theta) - u_z\sin\theta & u_xu_z(1-\cos\theta) + u_y\sin\theta \\ u_xu_y(1-\cos\theta) - u_z\sin\theta & \cos\theta + u_y^2(1-\cos\theta) & u_zu_y(1-\cos\theta) - u_x\sin\theta \\ u_zu_x(1-\cos\theta) - u_y\sin\theta & u_zu_y(1-\cos\theta) + u_x\sin\theta & \cos\theta + u_z^2(1-\cos\theta) \end{bmatrix}$$

Equations (51) come from the third column of $R(\theta)$. □

In hindsight, we could allow $v < 0$ in (51), so we can describe both twin circles in both directions. We have therefore *four* solutions, each twin pair passing starting at the north pole $(0, 0, r)$ with velocity vector $(v, 0, 0)$.

7 Numerical simulations

We are presently implementing two independent approaches, to validate each other. The first approach applies Pontryagin's method directly, with spherical coordinates $(\theta, \phi, v_\theta, v_\phi)$ in $TS^2(r)$ for the state equations. We use the freeware BOCOP developed

by F. Bonnan's group at INRIA, that has a built-in implicit equation solver to adjust the initial momenta. This freeware can be implemented also with euclidian coordinates constrained to the sphere. The second approach, uses a numerical ODE solver on our system (30,31). In future work, we will need to add an implicit equation solver, to find the initial momenta a, M_1, M_2, M_3 in order to reach the final position and velocities and the minimal time.

In order to mutually validate the two approaches. In (30, 31) we could add to the initial positions and velocities (known), the initial momenta M_1, M_2, M_3, a corresponding to the initial values of $p_\theta, p_\phi, p_{v_\theta}, p_{v_\phi}$ provided by the simulation with BOCOP. In "Appendix B" we derive the translating formulas between the two sets of momenta. We are planning for future work an in depth study, aiming a comparison between time minimal and cubic splines, using a set of representative initial and final positions and velocities.[4]

7.1 Using BOCOP (www.bocop.org)

Let's now summarize the first approach. We use letters θ, ϕ to parametrize the physical sphere $S^2(r)$ in the usual way

$$q = r\ (\cos\phi\cos\theta, \cos\phi\sin\theta, \sin\phi) \tag{53}$$

After straightforward calculations we get

$$\begin{aligned}\nabla_{\dot q}\dot q &= \left(r\cos\phi\,\ddot\theta - 2r\sin\phi\,\dot\theta\,\dot\phi\right)\,e_\theta + \left(r\ddot\phi + r\cos\phi\sin\phi\,\dot\theta^2\right)\,e_\phi\\ &= \bar u_1\,e_\theta + \bar u_2\,e_\phi\end{aligned} \tag{54}$$

with

$$e_\theta = (-\sin\theta, \cos\theta, 0)\,, \quad e_\phi = (-\sin\phi\cos\theta, -\sin\phi\sin\theta, \cos\phi)$$

and this gives us the state equations in $(\theta, \phi, v_\theta, v_\phi)$

$$\begin{aligned}\dot\theta &= v_\theta, \quad \dot\phi = v_\phi\\ \dot v_\theta &= 2\tan\phi \quad v_\theta\,v_\phi + \bar u_1/(r\cos\phi),\\ \dot v_\phi &= -\cos\phi\sin\phi\,v_\theta^2 + \bar u_2/r.\end{aligned} \tag{55}$$

It is nice to write the acceleration control in terms of the tangent and surface normal,

$$\bar u_1\,e_\theta + \bar u_2\,e_\phi = u_1\,\mathbf{t} + u_2\,\mathbf{n}$$

[4] We would like to lure a scientific initiation student for that.

where

$$\mathbf{t} = \frac{v_\theta \cos\phi}{\sqrt{v_\theta^2 \cos^2\phi + v_\phi^2}}\, e_\theta + \frac{v_\phi}{\sqrt{v_\theta^2 \cos^2\phi + v_\phi^2}}\, e_\phi$$
$$\mathbf{n} = -\frac{v_\phi}{\sqrt{v_\theta^2 \cos^2\phi + v_\phi^2}}\, e_\theta + \frac{v_\theta \cos\phi}{\sqrt{v_\theta^2 \cos^2\phi + v_\phi^2}}\, e_\phi$$

so that we just replace in (55) the controls $\bar{u}_1, \bar{u}_2$ by

$$\bar{u}_1 = u_1 \frac{v_\theta \cos\phi}{\sqrt{v_\theta^2 \cos^2\phi + v_\phi^2}} - u_2 \frac{v_\phi}{\sqrt{v_\theta^2 \cos^2\phi + v_\phi^2}}$$
$$\bar{u}_2 = u_1 \frac{v_\theta \cos\phi}{\sqrt{v_\theta^2 \cos^2\phi + v_\phi^2}} + u_2 \frac{v_\theta \cos\phi}{\sqrt{v_\theta^2 \cos^2\phi + v_\phi^2}} \tag{56}$$

A nice feature of BOCOP is its built-in implicit equation solver. For the time minimal problem it adjusts (by a shooting method) the four unknown momenta $(p_\theta, p_\phi, p_{v_\theta}, p_{v_\phi})$ at the initial time position and velocity, and finds the time interval T leading to the prescribed end position and end velocity vector.[5]

Due to the SO(3) symmetry, in the simulations the initial and final positions can be taken at the equator ($\phi = 0$), and the initial longitude also set at $\theta^o = 0$. Thus the data to be chosen are θ^f and the initial and final values of the velocities v_θ, v_ϕ. The implicit solver is a shooting method to reach $\theta^f, v_\theta^f, v_\phi^f$ in an unknown time T from the initial values $\theta^o = \phi^o = 0, v_\theta^o, v_\phi^o$.

Figure 1 shows the result of a benchmark simulation, with initial and final conditions in a circle with $k_g = 1$. A further interesting check is to compare the numerical results for the costates $p_\theta(t), p_\phi(t), p_{v_\theta}(t), p_{v_\phi}(t)$ provided by BOCOP with the theoretical prediction that can be computed using (69). We can provide a zipped file with the implementation for the interested reader. When all is debugged, and the 'build' command in the GUI is working, one just clicks the green arrow, and BOCOP does the job automatically.

```
EXIT: Optimal Solution Found.

Objective value

f(x*) = 2.221489e+00

Time taken : 10.50s

Optimization SUCCEEDED!
```

[5] At first sight there are 5 unknowns for the four implicit equations, but the momenta p_{v_θ}, p_{v_ϕ} act with a scale invariance and they behave as one unknown.

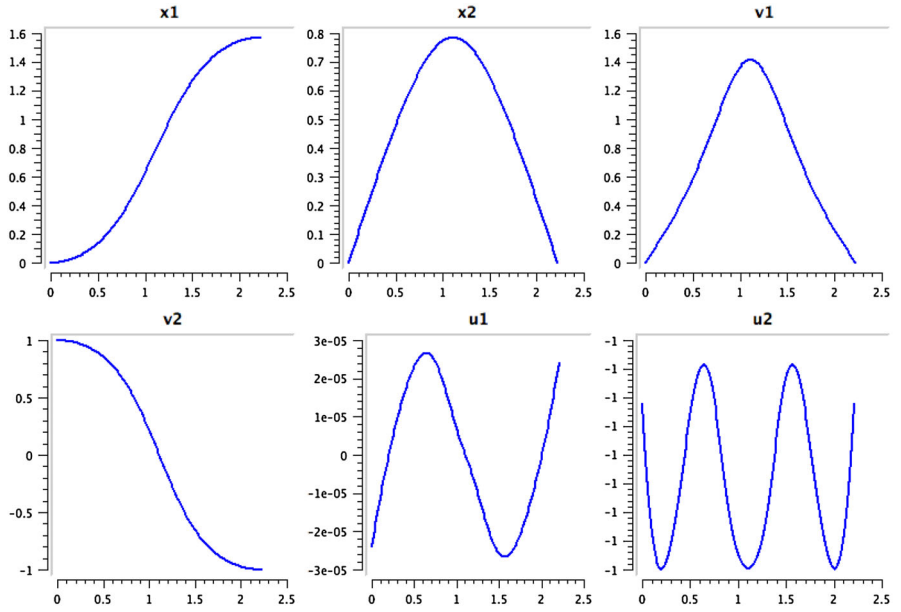

Fig. 1 Benchmark example. $x_1 = \theta, x_2 = \phi, v_1 = \dot{\theta}, v_2 = \dot{\phi}$; u_1, u_2 are respectively the tangential and normal accelerations; the boundary conditions are at half of a circle with $k_g = 1$: $\theta^o = \phi_o = 0, \dot{\theta}_o = 0, \dot{\phi}_o = 1, \theta_f = \pi/2, \phi_f = 0, \dot{\theta}_f = 0, \dot{\phi}_f = -1$. The control variables seem to oscillate, but note the scale: up to very small numerical error, $u_1 \equiv 0, u_2 \equiv 1$, as expected

Let us check if the time $T = 2.221489$ found by BOCOP is coherent with the theory. From (52) the difference $\sqrt{2} \times T - \pi$ must be equal to zero. Indeed, the result is 0.000067, a reasonable numerical error.

7.2 Using an ODE solver

The figures below depict numerical solutions for the Hamiltonian (41, 42) in variables a, v, z, θ, for a solution emanating from the unstable equilibrium with loxodromic eigenvalues. In Figs. 2, 3, 4 and, 5 the equilibrium is inserted as initial condition. As the program runs, the very small numerical error in the initial condition amplifies exponentially, and the solutions run away. Seemingly it approaches a neighborhood of the other organizing center corresponding to $|z| = 1$. Figures 6 and 7 hints on how intricate is phase portrait . Further numerical work will be needed to clarify the transition from the linear regime for very small t to the nonlinear regime, and the asymptotic behavior as $t \to \infty$, and if v reaches zero on such solutions.

8 Discussion

This paper is a follow up of [16]. The focus there was on a splitting of cotangent vectors $P_{(v,q)} \in T^*(TQ)$ and then rewriting the canonical symplectic form in these

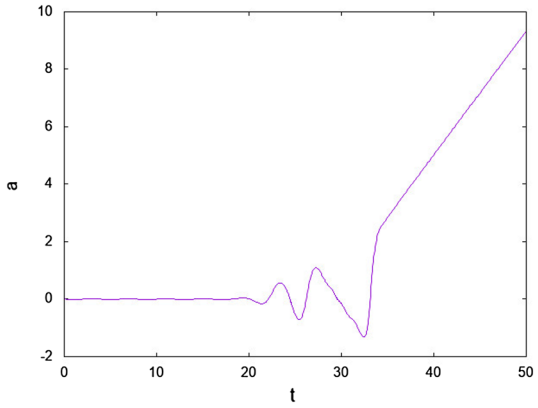

Fig. 2 $a - t$ plot for a solution emanating from the equilibrium. Parameters $r = A = 1$. Note the near linear evolution of $a(t)$ for larger values of t. The predicted slope, when $z \sim -1$ is $\dot{a} \sim \sqrt{2}$

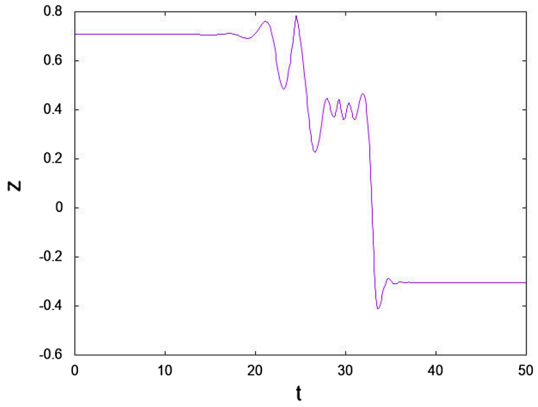

Fig. 3 $z - t$ plot. Note the dramatic change in sign of z around $t \sim 33$. For larger t it seems to stabilize far from $z = -1$

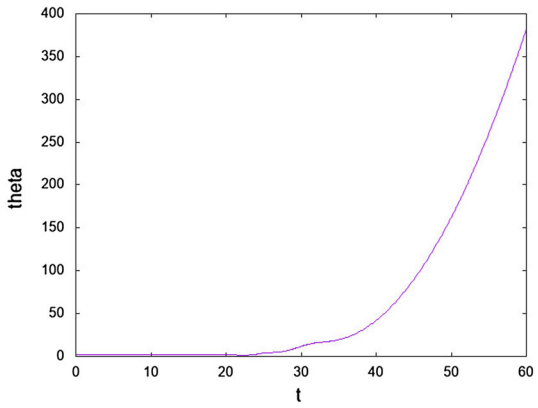

Fig. 4 $\theta - t$ plot. $\theta(t)$ controls the oscillations in the variables M_1, M_3 according to (39). Oscillations around the initial value $\theta_o = \pi/2$ are not visible due the large scales chosen

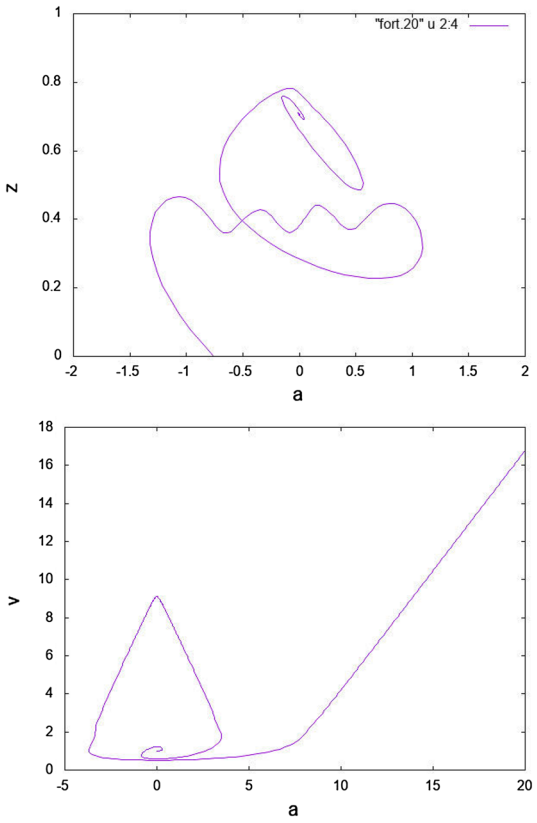

Fig. 5 $a - z$ and $a - v$ plots of the same solution of the previous figures

split coordinates. The main example was cubic splines on spheres: one fixes the time T, and minimizes the cost function $1/(2\beta)\int_O^T |\nabla_{\dot\gamma}\dot\gamma|^2 dt$. We gave a Hamiltonian formulation for the Crouch–Leite equations that generate the cubic splines on S^n (16). For $n = 2$, we used the coordinates $(v, R) \in TS^2 - 0$, and covectors $(a, M) \in T^*_{(v,R)}(TS^2 - 0)$ in order to study the reduced dynamics in (a, v, M) coordinates. We showed that the reduced cubic spline system is governed by the Hamiltonian

$$H^* = \frac{1}{2\beta}\left(a^2 + (M_3/v)^2\right) + M_2\, v/r.$$

In this paper we make a study about the time minimal splines with bounded acceleration on $S^2(r)$. As far as we know, this problem has not been addressed before. The same coordinates (v, R, a, M) are used here, leading to the reduced Hamiltonian

$$H^* = A\left(a^2 + (M_3/v)^2\right)^{1/2} + M_2\, v/r.$$

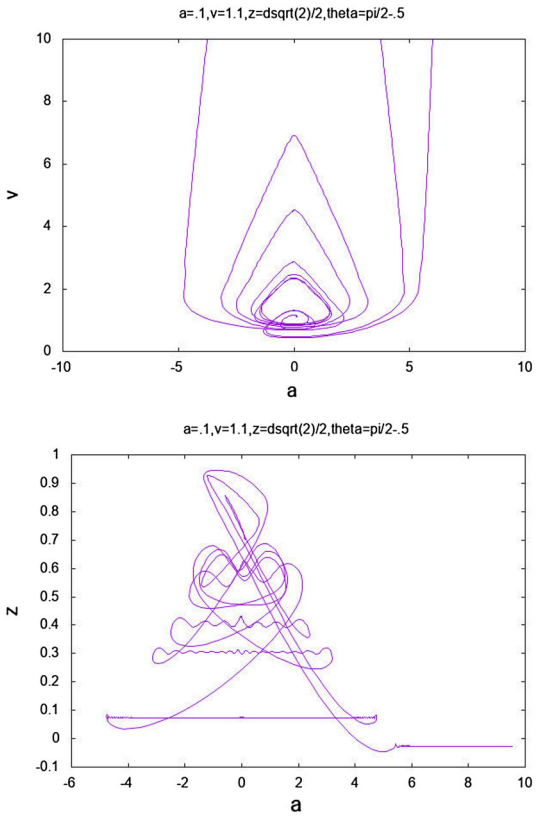

Fig. 6 Initial conditions appear in the top. Lagrangian projection $a - z$ and symplectic $a - v$ plane projection of the solution. The phase portrait becomes intricate as one leaves a small neighborhood of the unstable fixed point

The reduced equations are more involved with added subtleties. To start, here the costate a does not represent the tangential acceleration, as it was in the cubic spline case. We present in this discussion some loose ends and research directions.

8.1 Comparisons with cubic splines

It is curious that both reduced problems have the same loxodromic type of relative equilibria, and that the reconstructed paths are the same figure eights. Is there a reason beyond a mere mathematical coincidence? As regards to paths along the equators, the behavior is very different. For cubic splines the path obeys a third degree polynomial in time. For time minimal the path is a concatenation of two quadratic polynomials with a sudden jump on the second derivative, $\pm A$.

One problem that comes up for comparisons, is to study time minimal splines on the hyperbolic disk. It is known that on manifolds having regions of negative (sectional) curvature, cubic splines suffer a strange syndrome: the scalar velocity may reach infinity in finite time [29]. Time minimal splines offer an alternative if one needs to avoid this threat. Comparing trajectories, balancing the time spent vs. the energetic cost could be a topic for further research.

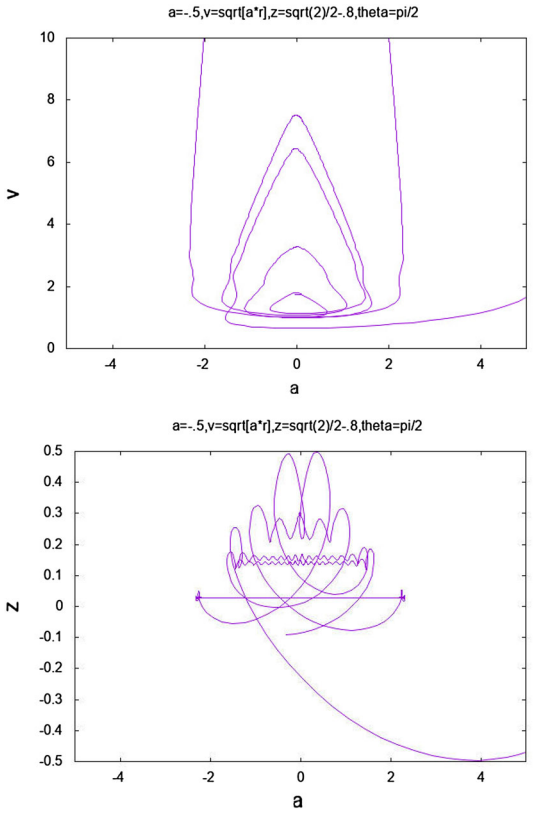

Fig. 7 Initial conditions on top on the figures. Lagrangian projection $a - z$ and symplectic $a - v$ plane projection of the solution

8.2 Invariant manifolds emanating from the equilibria

Recall from [16] that for cubic splines the union of relative equilibria solutions (all circles with $\kappa_g = 1/r$) forms a center manifold C of dimension 4. Each unreduced relative equilibrium trajectory can be associated to its initial position and velocity vector. This center manifold is parametrized by the base $\Re_+ \times SO(3) \equiv TS^2 - 0$. This is because the reduced equilibria have the scalar velocity v as a free parameter. In this case all nonzero momentum spheres have these relative equilibria trajectories. $M_1^2 + M_2^2 + M - 3^2 = \mu^2$, with $\mu = \sqrt{2}(\beta/r)\, v^3$. In the reduced space we have local unstable and stable (spiralling) manifolds of dimension two. They lift to 6-dimensional manifolds W_C^u, W_C^s inside $T^*(TS^2)$. This dimension count is coherent: $\dim C = 6 + 6 - 8 = 4$. There is a scale invariance, given by

$$(v(t), R(t)) \to (\gamma v(\gamma t), R(\gamma t)), \tag{57}$$

which for the conjugate momenta entails

$$a \to \gamma^2 a(\gamma t), \quad M \to \gamma^3 M(\gamma t). \tag{58}$$

For time minimal splines, there is a striking difference. The above scaling is lost, due to the interplay between the radius r and the acceleration A. In consequence, in the reduced system, *only one* momentum sphere $\mu = \sqrt{2A/r}$ has an equilibrium. Fix that momentum sphere, together with the total energy. Then the phase space has effective dimension 7. The center manifold is parametrized by $SO(3)$ since the velocity must be $\sqrt{Ar}$. The dimension count is $\dim C = 5 + 5 - 7 = 3$ which is also coherent. Global dynamical question can be posed for both cases: on the reduced system, take initial conditions near the loxodromic equilibrium. What happens with the corresponding reconstructed solutions? To start, it is in order understanding the global behavior of the 2-dimensional stable and unstable manifolds of the reduced system W^u_{red} and W^s_{red}. Do they intersect transversally?

8.3 Undefined situations for the controls

The time minimal spline problem in euclidian spaces has been addressed in [15,30–32]. Even in the plane, although the setting is quite simple, the analysis is subtle at special situations where the controls are undefined. Take x, v, p_x, p_v in $\Re^n$ ($n = 2$, and $n = 3$ suffice). The state equations are in this case $\dot{x} = v, \dot{v} = u$ so that the Hamiltonian family is

$$H = -1 + p_x \cdot v + p_v \cdot u, \quad |u| \leq A,$$

Hence $u^* = Ap_v/|p_v|$, provided $p_v \neq 0$. How the solutions behave when $p_v = 0$? This was discussed in the above references, but we fear that not completely settled.

The analysis in the sphere should be similar. Troublesome values of the reduced coordinates are i) $a = M_3 = 0$ with $v \neq 0$. and of course ii) $v = 0$. The value $v = 0$ is even more troublesome due to an artifact of the coordinates (v, R) in TS^2: R is not well defined at the zero section. Probably it will be useful in both cases to go back to the unreduced formulation (8, 9) at $\alpha = 0$.

Acknowledgements This work was supported by CAPES/CNPq grants from the Science without Frontiers program PVE11/2012 and PVE089/2013. We thank Maria Soledad Aronna and Pierre Martinon for her help with the software BOCOP. The time minimal spline problem on the sphere was implemented by students from the Summer Undergraduate Program PIBIC at the Mathematics Department of UFMG. JK thanks the colleagues Raphael Campos Drumond, Mario Jorge Carneiro, Sylvie Kamphorst, Sonia Carvalho for the invitation, and to Matthew Perlmutter for sharing the classes. He also wishes to thank the Organizing Committee and the colleagues at the Instituto Superior Tecnico for a wonderful meeting in honor of Prof. Waldyr Oliva.

Appendix A: Linearization at the equilbria

We take entries in the order v, a, θ, z. We have at the equilibria: $L = J\,\text{Hess}(H)$ where

$$J = \begin{pmatrix} 0 & 1 & 0 & 0 \\ -1 & 0 & 0 & 0 \\ 0 & 0 & 0 & 1/\mu \\ 0 & 0 & -1/\mu & 0 \end{pmatrix}, \quad \text{Hess}(H) = \begin{pmatrix} H_{vv} & H_{va} & H_{v\theta} & H_{vz} \\ H_{av} & H_{aa} & H_{a\theta} & H_{az} \\ H_{\theta v} & H_{\theta a} & H_{\theta\theta} & H_{\theta z} \\ H_{zc} & H_{za} & H_{z\theta} & H_{zz} \end{pmatrix}$$

so that

$$L = \begin{pmatrix} H_{av} & H_{aa} & H_{a\theta} & H_{az} \\ -H_{vv} & -H_{va} & -H_{v\theta} & -H_{vz} \\ H_{zv}/\mu & H_{za}/\mu & H_{z\theta}/\mu & H_{zz}/\mu \\ -H_{\theta v}/\mu & -H_{\theta a}/\mu & -H_{\theta\theta}/\mu & -H_{\theta z}/\mu \end{pmatrix}. \tag{59}$$

We get the four linearization matrices by substituting $\mu = \sqrt{2A/r}$ and

$$\begin{aligned} &a = 0, \quad v = \pm\sqrt{Ar} \\ &v > 0: \quad \theta = \pm\pi/2, \phi = \pi/4 \quad (z = \sqrt{2}/2) \\ &v < 0: \quad \theta = \pm\pi/2, \phi = -\pi/4 \quad (z = -\sqrt{2}/2) \end{aligned}$$

on the bank of derivatives below. They all give the same matrix L in (45).

Bank of derivatives. Denoting for short $P = a^2 + \frac{\mu^2(1-z^2)(\sin(\theta))^2}{v^2}$ we have:

$$\begin{aligned}
H_{aa} &= -Aa^2 P^{-3/2} + A\, P^{-1/2} \\
H_{vv} &= -\frac{A\mu^4\left(1-z^2\right)^2(\sin(\theta))^4}{v^6} P^{-3/2} \\
&\quad + 3\,\frac{A\mu^2\left(1-z^2\right)(\sin(\theta))^2}{v^4} P^{-1/2} \\
H_{zz} &= -\frac{A\mu^4 z^2(\sin(\theta))^4}{v^4} P^{-3/2} - \frac{A\mu^2(\sin(\theta))^2}{v^2} P^{-1/2} \\
H_{\theta\theta} &= -\frac{A\mu^4\left(1-z^2\right)^2(\sin(\theta))^2(\cos(\theta))^2}{v^4} P^{-3/2} \\
&\quad + \frac{A\mu^2\left(1-z^2\right)(\cos(2\theta))^2}{v^2} P^{-1/2} \\
H_{av} &= \frac{Aa\mu^2\left(1-z^2\right)(\sin(\theta))^2}{v^3} P^{-3/2} \\
H_{a\theta} &= -\frac{Aa\mu^2\left(1-z^2\right)\sin(\theta)\cos(\theta)}{v^2} P^{-3/2} \\
H_{\theta z} &= \frac{A\mu^4 z(\sin(\theta))^3\left(1-z^2\right)\cos(\theta)}{v^4} P^{-3/2} - 2\,\frac{A\mu^2 z\sin(\theta)\cos(\theta)}{v^2} P^{-1/2} \\
H_{v\theta} &= \frac{A\mu^4\left(1-z^2\right)^2(\sin(\theta))^3\cos(\theta)}{v^5} P^{-3/2} \\
&\quad - 2\,\frac{A\mu^2\left(1-z^2\right)\sin(\theta)\cos(\theta)}{v^3} P^{-1/2} \\
H_{az} &= \frac{Aa\mu^2 z\,(\sin(\theta))^2}{v^2} P^{-3/2} \\
H_{vz} &= -\frac{Aa\mu^2\left(1-z^2\right)\sin(\theta)\cos(\theta)}{v^2} P^{-3/2}
\end{aligned}$$

Appendix B: Dictionary between the momenta in $T^*(TS^2)$ associated to the coordinate systems on TS^2

We derive the correspondence p_θ, p_ϕ, p_{v_θ}, p_{v_ϕ} to (a, M_1, M_2, M_3) that may be useful in future work. Let $Z(\alpha)$ denote the rotation about the z axis of and angle α and $Y(\beta)$ about the y axis of angle β. We introduce Euler angles ξ_1, ξ_2, ξ_3, for matrices $R \in SO(3)$ so that

$$\begin{aligned} R &= Z(\xi_1)\, Y(\pi/2 - \xi_2)\, Z(\xi_3) \\ &= \begin{pmatrix} c_1 s_2 c_3 - s_1 s_3 & -c_3 s_1 - c_1 s_2 s_3 & c_1 c_2 \\ c_1 s_3 + s_2 c_3 s_1 & c_1 c_3 - s_2 s_1 s_3 & s_1 c_2 \\ -c_3 c_2 & c_2 s_3 & s_2 \end{pmatrix} \end{aligned} \tag{60}$$

with $-\pi \le \xi_1, \xi_3 \le \pi, -\pi/2 \le \xi_2 \le \pi/2$. This is one among many possible parametrizations. We interchanged in Y the cosines with sines in order to the third column of R to have the same entries as the with θ, ϕ of the spherical coordinates, identifying them with Euler angles 1,2 respectively. Recall the map $SO(3) \times \Re_+ \to TS^2 - 0$. Since the normalized velocity vector is the first column R^1, we have $v_\theta (r\, \cos\phi) = v\, e_\theta \cdot R^1$, $\quad v_\phi\, r = v\, e_\phi \cdot R^1$. It results that the mapping $(v, \xi_1, \xi_2, \xi_3) \mapsto (\theta, \phi, v_\theta, v_\phi)$ is given by

$$\theta = \xi_1, \quad \phi = \xi_2\,, \quad v_\theta = \frac{v\, \sin\xi_3}{r\, \cos\xi_2}, \quad v_\phi = -\frac{v \cos(\xi_3)}{r}. \tag{61}$$

and can be easily inverted:

$$\xi_3 = -\arctan(\cos(\phi) v_\theta / v_\phi), \quad v = r\sqrt{\cos^2(\phi) v_\theta^2 + v_\phi^2}\,. \tag{62}$$

The conjugate momenta can be related by the pullback of the canonical 1-form in $T^*(TS^2)$:

$$a\, dv + p_{\xi_1}\, d\xi_1 + p_{\xi_2}\, d\xi_2 + p_{\xi_3}\, d\xi_3 = p_\theta\, d\theta + p_\phi\, d\phi + p_{v_\theta}\, dv_\theta + p_{v_\phi}\, dv_\phi \tag{63}$$

Computing the differentials $d\theta, d\phi, dv_\theta, dv_\phi$ from (61) and inserting in the RHS of the above identity, and collecting terms, one gets for a, p_{ξ_1}, p_{ξ_2}, p_{ξ_2} linear functions of p_θ, p_ϕ, p_{v_θ}, p_{v_ϕ} with coefficients depending on $\theta = \xi_1, \phi = \xi_2, \xi_3, v$. The result is

$$\begin{bmatrix} p_{\xi_1} \\ p_{\xi_2} \\ p_{\xi_3} \\ a \end{bmatrix} = \begin{bmatrix} 1 & 0 & 0 & 0 \\ 0 & 1 & -\frac{v\, s_3\, s_2}{r\, c_2^2} & 0 \\ 0 & 0 & \frac{v\, c_3}{r\, c_2} & \frac{v\, s_3}{r} \\ 0 & 0 & \frac{s_3}{r\, c_2} & -\frac{c_3}{r} \end{bmatrix} \begin{bmatrix} p_\theta \\ p_\phi \\ p_{v_\theta} \\ p_{v_\phi} \end{bmatrix} \tag{64}$$

A second step consists on relating (M_1, M_2, M_3) with $(p_{\xi_1}, p_{\xi_2}, p_{\xi_3})$. We start with the identity in $T^*SO(3)$

$$p_{\xi_1} d\xi_1 + p_{\xi_2} d\xi_2 + p_{\xi_3} d\xi_3 = M_1\, \Omega_1 + M_2\, \Omega_2 + M_2\, \Omega_3 \tag{65}$$

where the Ω_i are differential forms that can be expressed in terms of the $d\xi_1, d\xi_2, d\xi_3$, via the very classical expressions (going back to Euler) that come from

$$R^{-1} dR = [\Omega] = \begin{pmatrix} 0 & -\Omega_3 & \Omega_2 \\ \dots & 0 & -\Omega_1 \\ \dots & \dots & 0 \end{pmatrix}.$$

A long but straightforward computation, or a fast computer algebra (we did it on Maple), gives well known formulae for the infinitesimal rotations in the body frame:

$$\begin{aligned} \Omega_1 &= -\cos(\xi_3)\, \cos(\xi_2)\, d\xi_1 - \sin(\xi_3)\, d\xi_2 \\ \Omega_2 &= \cos(\xi_2)\, \sin(\xi_3)\, d\xi_1 - \cos(\xi_3)\, d\xi_2 \\ \Omega_3 &= \sin(\xi_2)\, d\xi_1 + d\xi_3 \end{aligned} \tag{66}$$

which gives

$$\begin{aligned} p_{\xi_1} &= -M_1 \cos(\xi_3) \cos(\xi_2) + M_2 \cos(\xi_2) \sin(\xi_3) + M_3\, \sin(\xi_2) \\ p_{\xi_2} &= -\sin(\xi_3)\, M_1 - \cos(\xi_3)\, M_2 \\ p_{\xi_3} &= M_3 \end{aligned} \tag{67}$$

Inverting these linear relations we get

$$\begin{bmatrix} M_1 \\ M_2 \\ M_3 \\ a \end{bmatrix} = \begin{bmatrix} -c_3/c_2 & -s_3 & s_2 c_3/c_2 & 0 \\ s_3/c_2 & -c_3 & -s_2 s_3/c_2 & 0 \\ 0 & 0 & 1 & 0 \\ 0 & 0 & 0 & 1 \end{bmatrix} \begin{bmatrix} p_{\xi_1} \\ p_{\xi_2} \\ p_{\xi_3} \\ a \end{bmatrix} \tag{68}$$

Multiplying the matrices in (64, 68) one obtains the desired correspondence

$$\begin{bmatrix} M_1 \\ M_2 \\ M_3 \\ a \end{bmatrix} = \begin{bmatrix} -\frac{c_3}{c_2} & -s_3 & \frac{v s_2}{r\, c_2^2} & \frac{v s_2 s_3 c_3}{r\, c_2} \\ \frac{s_3}{c_2} & -c_3 & 0 & -\frac{v s_2 s_3^2}{r\, c_2} \\ 0 & 0 & \frac{v\, c_3}{r\, c_2} & \frac{v s_3}{r} \\ 0 & 0 & \frac{s_3}{r\, c_2} & -\frac{c_3}{r} \end{bmatrix} \begin{bmatrix} p_\theta \\ p_\phi \\ p_{v_\theta} \\ p_{v_\phi} \end{bmatrix} \tag{69}$$

The reader may further wish to change to the split momenta coordinates, in this case just changing to, according to [16] [with v_θ from (61)]

$$\hat{p}_\theta = p_\theta - \cos(\phi)\sin(\phi)v_\theta p_{v_\phi},\ \hat{p}_\phi = p_\phi + 2\tan(\phi)v_\theta p_{v_\theta}. \tag{70}$$

References

1. Francis, B., Maggiore, M.: Flocking and Rendezvous in Distributed Robotics. Springer, New York (2016)
2. Smith, S., Broucke, M., Francis, B.: Curve shortening and the rendezvous problem for mobile autonomous robots. IEEE Trans. Autom. Control **52**(6), 1154 (2007). https://doi.org/10.1109/TAC.2007.899024
3. Lin, Z., Francis, B., Maggiore, M.: Getting mobile autonomous robots to rendezvous. In: Francis, B.A., Smith, M.C., Willems, J.C. (eds.) Control of Uncertain Systems: Modelling, Approximation, and Design. Lecture Notes in Control and Information Sciences, vol. 329. Springer-Verlag, Berlin, Heidelberg (2006)
4. Weyr, A.: The Martian. Broadway Books, Portland (2014)
5. Lewis, A.D.: Aspects of geometric mechanics and control of mechanical systems. Ph.D. thesis, Caltech. http://www.mast.queensu.ca/~andrew/papers/pdf/1995f.pdf (1995)
6. Bullo, F., Lewis, A.D.: Geometric Control of Mechanical Systems. Texts in Applied Mathematics, vol. 49. Springer, New York (2005)
7. Noakes, L., Heinzinger, G., Paden, B.: Cubic splines on curved spaces. IMA J. Math. Control Inf. **6**(4), 465 (1989). https://doi.org/10.1093/imamci/6.4.465
8. Crouch, P., Leite, F.S.: Geometry and the dynamic interpolation problem. In: Proceedings of the 1991 American Control Conference, pp. 1131–1136 (1991)
9. Younes, L.: Shapes and Diffeomorphisms. Applied Mathematical Sciences, vol. 171. Springer, New York (2010)
10. Singh, N., Niethammer, M.: Splines for diffeomorphic image regression. In: Golland, P., Hata, N., Barillot, C., Hornegger, J., Howe, R. (eds.) Medical Image Computing and Computer-Assisted Intervention–MICCAI 2014. Lecture Notes in Computer Science, vol. 8674, pp. 121–129. Springer (2014). https://doi.org/10.1007/978-3-319-10470-6_16
11. Fiot, J.B., Raguet, H., Risser, L., Cohen, L.D., Fripp, J., Vialard, F.X.: Longitudinal deformation models, spatial regularizations and learning strategies to quantify Alzheimer's disease progression. NeuroImage Clin. **4**, 718 (2014). https://doi.org/10.1016/j.nicl.2014.02.002. http://www.sciencedirect.com/science/article/pii/S2213158214000205
12. Durrleman, S., Fletcher, T., Gerig, G., Niethammer, M., Pennec, X.: Spatio-Temporal Image Analysis for Longitudinal and Time-Series Image Data. Lecture Notes in Computer Science, vol. 8682. Springer, Cambridge (2015). https://doi.org/10.1007/978-3-319-14905-9
13. Kaya, C.Y., Noakes, J.L.: Finding interpolating curves minimizing L^∞ acceleration in the Euclidean space via optimal control theory. SIAM J. Control Optim. **51**(1), 442 (2013). https://doi.org/10.1137/12087880X
14. Noakes, L.: Minimum L^∞ accelerations in Riemannian manifolds. Adv. Comput. Math. **40**(4), 839 (2014). https://doi.org/10.1007/s10444-013-9329-9
15. Castro, A.L., Koiller, J.: On the dynamic Markov-Dubins problem: from path planning in robotics and biolocomotion to computational anatomy. Regul. Chaotic Dyn. **18**(1–2), 1 (2013). https://doi.org/10.1134/S1560354713010012
16. Balseiro, P., Stuchi, T., Cabrera, A., Koiller, J.: About simple variational splines from the Hamiltonian viewpoint. J. Geom. Mech. **9**(3), 257–290 (2017). https://doi.org/10.3934/jgm.2017011
17. Popiel, T.: Mathematics of control. Signals Syst. **19**(3), 235 (2007). https://doi.org/10.1007/s00498-007-0012-x
18. Hinkle, J., Muralidharan, P., Fletcher, P., Joshi, S.: Polynomial regression on Riemannian Manifolds. In: Fitzgibbon, A., Lazebnik, S., Perona, P., Sato, Y., Schmid, C. (eds.) Computer Vision—ECCV 2012. Lecture Notes in Computer Science, vol. 7574, pp. 1–14. Springer, Berlin (2012). https://doi.org/10.1007/978-3-642-33712-3_1

19. Hinkle, J., Fletcher, P., Joshi, S.: Intrinsic polynomials for regression on Riemannian manifolds. J. Math. Imaging Vis. **50**(1–2), 32 (2014). https://doi.org/10.1007/s10851-013-0489-5
20. Burnett, C.L., Holm, D.D., Meier, D.M.: Inexact trajectory planning and inverse problems in the Hamilton–Pontryagin framework. Proc. R. Soc. Lond. A Math. Phys. Eng. Sci. (2013). https://doi.org/10.1098/rspa.2013.0249
21. Gay-Balmaz, F., Holm, D.D., Meier, D.M., Ratiu, T.S., Vialard, F.X.: Invariant higher-order variational problems. Commun. Math. Phys. **309**(2), 413 (2012). https://doi.org/10.1007/s00220-011-1313-y
22. Gay-Balmaz, F., Holm, D.D., Meier, D.M., Ratiu, T.S., Vialard, F.X.: Invariant higher-order variational problems II. J. Nonlinear Sci. **22**(4), 553 (2012). https://doi.org/10.1007/s00332-012-9137-2
23. Niethammer, M., Huang, Y., Vialard, F.X.: Geodesic regression for image time-series. In: Fichtinger, G., Martel, A., Peters, T. (eds.) Medical Image Computing and Computer-Assisted Intervention—MICCAI 2011. Lecture Notes in Computer Science, vol. 6892, pp. 655–662. Springer, Berlin (2011). https://doi.org/10.1007/978-3-642-23629-7_80
24. Steinke, F., Hein, M., Schölkopf, B.: Nonparametric regression between general Riemannian manifolds. SIAM J. Imaging Sci. **3**(3), 527 (2010). https://doi.org/10.1137/080744189
25. Desai, N., Ploskonka, S., Goodman, L.R., Austin, C., Goldberg, J., Falcone, T.: Analysis of embryo morphokinetics, multinucleation and cleavage anomalies using continuous time-lapse monitoring in blastocyst transfer cycles. Reproduct. Biol. Endocrinol. RB&E **12**, 54 (2014). https://doi.org/10.1186/1477-7827-12-54
26. Chang, D.E.: A simple proof of the Pontryagin maximum principle on manifolds. Automatica **47**(3), 630 (2011). https://doi.org/10.1016/j.automatica.2011.01.037. http://www.sciencedirect.com/science/article/pii/S0005109811000525
27. Crouch, P., Leite, F.: The dynamic interpolation problem: on Riemannian manifolds, Lie groups, and symmetric spaces. J. Dyn. Control Syst. **1**(2), 177 (1995). https://doi.org/10.1007/BF02254638
28. Intriligator, M.D.: Mathematical Optimization and Economic Theory. Classics in Applied Mathematics, vol. 39. SIAM, Philadelphia (2002)
29. Pauley, M., Noakes, L.: Cubics and negative curvature. Differ. Geom. Appl. **30**(6), 694 (2012). https://doi.org/10.1016/j.difgeo.2012.09.004
30. Johnson, S.D.: Computing minimum time paths with bounded acceleration. arXiv:1310.5905 [math.NA] (2013)
31. Carozza, D., Johnson, S., Morgan, F.: Baserunner's optimal path. Math. Intell. **32**(1), 10 (2010). https://doi.org/10.1007/s00283-009-9106-2
32. Venkatraman, A., Bhat, S.P.: Optimal planar turns under acceleration constraints. In: Proceedings of the 45th IEEE Conference on Decision and Control, pp. 235–240 (2006). https://doi.org/10.1109/CDC.2006.377809